Fragmentation of the Valence Electronic States of CF_3Cl^+ and CF_3Br^+ Studied by Threshold Photoelectron–Photoion Coincidence Spectroscopy

ARTICLE *in* THE JOURNAL OF PHYSICAL CHEMISTRY · MARCH 1996

Impact Factor: 2.78 · DOI: 10.1021/jp952318x

6 AUTHORS, INCLUDING:

Richard P Tuckett
University of Birmingham
162 PUBLICATIONS **2,058** CITATIONS

Fragmentation of the Valence Electronic States of CF_3Cl^+ and CF_3Br^+ Studied by Threshold Photoelectron−Photoion Coincidence Spectroscopy

Jeremy C. Creasey, David M. Smith, Richard P. Tuckett,* and Karl R. Yoxall

School of Chemistry, University of Birmingham, Edgbaston, Birmingham B15 2TT, U.K.

Keith Codling and Paul A. Hatherly

Department of Physics, University of Reading, Whiteknights, Reading RG6 2AF, U.K.

Received: May 30, 1995; In Final Form: December 6, 1995[⊗]

Using tunable vacuum-UV radiation from a synchrotron source, fragmentation studies have been performed on the valence states of CF_3Cl^+ and CF_3Br^+ in the energy range 10−25 eV both with and without energy state selectivity of the photoelectrons. In the latter case, thresholds and yield curves are obtained for the parent and fragment ions, and the results agree well with complementary studies of other groups. In the former case, threshold photoelectron−photoion coincidence (TPEPICO) spectroscopy is used to measure the decay pathways of individual valence states of CF_3X^+ (X = Cl, Br). TPEPICO spectra are recorded both continuously as a function of photon energy, allowing threshold photoelectron spectra and yields of the fragment ions to be obtained, and at a fixed photon energy with good time resolution, allowing mean translational kinetic energy releases, $\langle KE \rangle_t$, to be measured. $\langle KE \rangle_t$ values are measured at the Franck−Condon maxima of the valence states of CF_3X^+, substantially extending the earlier work of Powis (*Mol. Phys.* **1980**, *39*, 311). The CF_3X molecules are not big enough to belong to the 'large molecule' limit. By comparing the $\langle KE \rangle_t$ values with those predicted for the limiting extremes of a statistical and an impulsive dissociation process, some information on the nature of the photodissociation dynamics can be inferred. All the first four excited states ($\tilde{A}\ ^2A_1$, $\tilde{B}\ ^2A_2$, $\tilde{C}\ ^2E$, and $\tilde{D}\ ^2E$) of CF_3X^+, where dissociation occurs by loss of an F or X atom, show evidence of isolated-state behavior, and the $\langle KE \rangle_t$ values suggest that there is a relationship between the part of the parent molecule where ionization occurs and the bond that breaks to form the fragment ion + atom products. Statistical values of $\langle KE \rangle_t$ are most likely when ionization occurs at a part of the molecule furthest away from the bond that breaks. Conversely, impulsive (and hence larger) values of $\langle KE \rangle_t$ are more likely when the breaking bond lies close to the part of the molecule where ionization occurs.

1. Introduction

Halogenated methanes have important applications in many areas of technology, ranging from the fabrication of semiconductors by plasma etching[1] to their use as refrigerants. However, the harmlessness of these compounds which make them so attractive for lab-based technology is lost as they diffuse into the stratosphere where they undergo solar UV photodissociation. For the chlorinated methanes, the free Cl atoms liberated in this process are of major significance in the catalytic depletion of stratospheric ozone.[2] The UV and vacuum-UV photochemistry of these molecules has therefore aroused much interest, and an understanding of the decay dynamics of valence and Rydberg states of the neutral molecule and excited valence states of the parent molecular ion can provide useful information for atmospheric modelers. Whilst the UV photodissociation of many of the freons has been extensively studied, there has been less work on the vacuum-UV photodissociation processes that occur. Yet, despite the fact that only a very small amount of the freons will avoid UV photodissociation in the stratosphere, some will diffuse higher up into the ionosphere where more vacuum-UV radiation (especially Lyman-α at 121.6 nm) is present, and it is important to know the fate of freon molecules under these conditions. In this paper we use a coincidence technique involving the detection of threshold photoelectrons to measure the unimolecular decay dynamics of the valence states of CF_3Cl^+ and CF_3Br^+.

The two freons CF_3Cl and CF_3Br have been studied by He I and He II photoelectron spectroscopy,[3,4] techniques which establish the ionization energies and nature of the valence molecular orbitals (MOs) for these molecules. Prior to this work, a threshold, zero energy photoelectron spectrum has only been reported for CF_3Cl.[5] Previous quantitative investigations of the fragmentation of CF_3-containing ions in the vacuum-UV have concentrated on CF_3Cl^+, with correspondingly scarce data for CF_3Br^+. Both photoionization mass spectrometry (PIMS)[5−7] and 'pseudophoton' dipole (e, e + ion) spectroscopy[8] have been used to measure appearance potentials and ionic fragmentation branching ratios for CF_3Cl^+, but these are *not* state-specific techniques, and no meaningful information on the dissociation dynamics (*e.g.* measurements of the kinetic energy (KE) released into translation of the products) was obtained. There have been two corresponding PIMS studies of CF_3Br.[6,9] The only state-selected experiments on CF_3Cl^+ and CF_3Br^+ reported are due to Powis *et al.*,[10,11] where a He I photoelectron−photoion coincidence (PEPICO) technique was used to investigate the unimolecular dissociation of some of the valence states of CF_3Cl^+ and CF_3Br^+. More data was reported for CF_3Cl^+, and it was commented that CF_3Br had a deleterious effect on the microchannel plate ion detector. The valence states of CF_3Cl^+ and CF_3Br^+ which were studied showed a mixture of statistical and direct dissociation mechanisms, with some evidence for isolated-state behavior. Similar results have more recently been reported by Lane and Powis[12] for the dissociation of the ground and first two excited valence states of CH_3Cl^+ and CH_3Br^+,

[⊗] Abstract published in *Advance ACS Abstracts,* February 15, 1996.

0022-3654/96/20100-4350$12.00/0

where again a mixture of statistical and state-specific dynamical dissociation mechanisms was discovered.

In this paper we report measurements on CF_3Cl^+ and CF_3Br^+ using two complementary techniques. In both cases tunable vacuum-UV photons from a synchroton are the source of electromagnetic radiation. One uses an electron−ion coincidence technique,[13] but in which there is no energy state-selectivity of the electrons. (We deliberately do not call this a PEPICO experiment because the energy of the photoelectrons is not defined.) This experiment effectively gives ion yield curves and thresholds for the production of fragment ions, data similar to PIMS studies, but because the internal energy of the parent ion is not defined the translational KE releases cannot be interpreted meaningfully. Preliminary results have been reported briefly elsewhere.[14] The second uses a threshold photoelectron−photoion coincidence (TPEPICO) technique,[15] in which zero energy electrons are detected in coincidence with ions separated by time-of-flight mass spectrometry. This *is* a state-selected experiment and allows the fragmentation channels of individual electronic states of the parent ion to be studied. The fragment ions that are observed and the KE released into these channels are important guides to statistical or dynamical behavior in the different electronic states of the parent ion. Finally in this Introduction, we comment that the phrase 'state selection' in this paper essentially refers to the selection of a particular *electronic* state of the parent ion. It does not refer to vibrational or rovibrational state selectivity, as has now been achieved by other higher-resolution techniques.

2. Experimental Details

The experiments were performed at the U.K. Synchrotron Radiation Source at Daresbury. Synchrotron radiation is dispersed using either a 1 m Seya−Namioka (in this paper abbreviated to Seya) or a 5 m normal-incidence McPherson monochromator. Both cover the wavelength range 300−1200 Å or *ca*. 10−40 eV. The dispersed vacuum-UV radiation is introduced into one of two stainless-steel chambers via a 100 mm long, 2 mm i.d. glass capillary and monitored by a window coated with sodium salicylate and a photomultiplier tube which allows for flux normalization. The photoionization yield curves for both CF_3Cl and CF_3Br were obtained using the Seya monochromator at a band-pass of 4 Å. The grating used has a range 400−1100 Å and is blazed at *ca*. 580 Å, and second-order radiation is only a slight problem for $\lambda > 1000$ Å. The majority of the state-specific TPEPICO experiments for CF_3Cl were carried out using the Seya monochromator, but all the CF_3Br experiments and some of the fixed-energy CF_3Cl experiments (see below) used the McPherson monochromator at a band-pass of 2 Å.

The photoionization yield curves were obtained using an electron−ion coincidence apparatus which has been described in detail elsewhere.[13] Essentially, it comprises two identical time-of-flight (TOF) drift tubes (field-free region 70 mm long) which lie orthogonal to and equidistant from the direction of the vacuum-UV photon beam. An extraction field of 78.5 V cm^{-1} accelerates electrons into one tube and ions into the other, and the photoionization products are detected by two pairs of microchannel plates (Galileo-MCP 40/32). The grid configuration and potentials in the TOF tubes satisfy the space-focusing condition.[16] Correlated electrons and ions from the same ionization event are detected in delayed coincidence. The TOF data are processed using CAMAC electronics, and the experiment is controlled by two interacting computers. An IBM-PC/AT sets the experimental parameters, displays the data in real time, and stores it on disk. A station PC scans the grating in the Seya monochromator and stores the total electron and ion signals (amongst other auxilliary data). Flux normalization is achieved by recording coincidences at a particular photon wavelength until the accumulated counts from the photomultiplier reach a preset value. The excitation wavelength is then stepped on and the process repeated. Data thus accumulate as a three-dimensional histogram of photon wavelength *vs* ion TOF *vs* coincidences. Suitable cuts through the histogram can then produce the ion yield curves which are shown in this paper. We believe that the principal advantage of TOF mass spectrometry of this kind over other sorts of ion detector (*e.g*. a quadrupole mass spectrometer which is commonly used in PIMS studies) is that *all* the ions are detected simultaneously in a single experiment, allowing fragment ion branching ratios to be determined at any vacuum-UV wavelength. Used in conjunction with a quasi-continuous excitation source, this apparatus allows thresholds for production of the different fragment ions to be measured with an accuracy only limited by the band-pass of the dispersive monochromator. Its principal limitation is that there is no energy analysis of the electrons, and in effect they are just used to provide the 'start' signal for the coincidence experiment. The electrons can therefore originate from photoionization of CF_3X to several electronic states of the parent ion, making this a non-state-specific experiment. We note that with this apparatus Stankiewicz *et al*.[17] estimate that electrons are collected with 100% efficiency so long as their kinetic energy < 7.9 eV. Similarly, ions (irrespective of their mass) are all collected if their kinetic energy < 8.8 eV.

The state-specific TPEPICO apparatus has also been described in detail elsewhere.[15] The same methods of flux normalization, electronics, and data collection are used as above. The two identical 70 mm drift tubes are now replaced by a threshold electron analyzer with a resolution of *ca*. 4 meV and a longer ion TOF drift tube (field-free region now 186 mm long), allowing for improved mass resolution. The threshold electron analyzer incorporates a cylindrical electrostatic lens designed with large chromatic aberrations, followed by a 127° postanalyzer which rejects the energetic electrons on the axis. Even with an extraction field as large as 20 V cm^{-1}, simulations[15] and experiments[18] confirm that this analyzer has both high efficiency (*ca*. 30% for zero energy electrons) and good resolution (*ca*. 4 meV). As in the apparatus described above, the ion detector consists of a two-stage acceleration region and a field-free region configured to satisfy space focusing. This allows the measurement of the KE release from a dissociative ionization process whilst still retaining a high ion collection efficiency. The electron and ion signals are now collected by a channeltron electron multiplier (Phillips X818BL) and a pair of microchannel plates (Galileo MCP-40/32), respectively. The raw pulses are passed to discriminator and pulse-shaping circuits (based on the LeCroy HVL 100 discriminator) and fed into a LeCroy 4208 time-to-digital converter (TDC) configured in the 'multihit' mode. The threshold electrons provide the start pulses, the ions provide the stop pulses, and the two signals from the same ionization event are detected in delayed coincidence, yielding a TPEPICO spectrum. All experiments use the 'multibench' quasi-continuous mode of the synchrotron source, and pulsed extraction is not used for either electron or ion detection. Three types of experiment can be performed. First, a threshold photoelectron spectrum (TPES) of the sample gas can be measured, simply by recording the threshold electron signal as a function of photon wavelength or energy. Second, a TPEPICO spectrum can be recorded at a fixed photon energy. In order to obtain the best possible kinetic energy release distribution (KERD),[19] TOF data accumulate at as high a time

resolution of the TDC as the signal level will permit. Third, a TPEPICO spectrum can be recorded continuously as a function of photon wavelength, using the method of flux normalization described above. Usually, *all* the ions produced in the TPEPICO spectrum are recorded in this energy-scanning mode, and the resolution of the TDC is correspondingly degraded. Ion yields are obtained as described above. Because the threshold electron signal is also recorded by the computer that controls the scanning of the monochromator, a TPES can be displayed simultaneously with the yields of the fragment ions, and this is how the data are presented in this paper.

CF_3Cl and CF_3Br gases (Aldrich Ltd.) were used without further purification. The gas under study effuses through a 0.5 mm i.d. stainless-steel needle whose tip is located *ca*. 25 mm from the center of the interaction region. Under these conditions we find that there is no axial or translational cooling of the molecules,[15] and to analyze the KE releases an axial translational temperature of 300 K is assumed. The base pressure of either apparatus is typically 1×10^{-7} Torr, while the background pressure during an experiment is between 3×10^{-5} and 1×10^{-4} Torr. Over this range we find that the shapes of the fixed-energy TPEPICO spectra are invariant to pressure, indicating that the effects of ion−molecule collisions are not significant over the time scale of the experiment.

Recent vacuum-UV fluorescence excitation experiments at Daresbury[20] suggested that the fifth excited state of CF_3Cl^+, $\tilde{E}\ ^2A_1$, shows weak radiative decay. For CF_3Br[21] UV/visible fluorescence was observed for an excitation energy of *ca*. 20 eV, the energy of the $\tilde{E}\ ^2A_1$ ionic state, but there was some doubt as to whether the emission is due to CF_3Br^+ or a fragment species. These hypotheses have been confirmed by threshold photoelectron−fluorescence coincidence experiments which will be described in a future paper.[22] We confirm that the fluorescence quantum yield of this state of the parent ions is too small to measure in CF_3Br^+ and is probably on the order of 10^{-1} to 10^{-2} in CF_3Cl^+. This radiative channel makes very little difference to the analysis of the TPEPICO and KERD results presented in this paper.

3. Energetics and Dissociation Channels of CF_3Cl^+ and CF_3Br^+

In C_{3v} geometry the electron configuration of the eight highest-occupied outer valence molecular orbitals (MOs) of CF_3Cl and CF_3Br is $...(3a_1)^2(2e)^4(4a_1)^2(3e)^4(4e)^4(1a_2)^2(5a_1)^2(5e)^4$, where the numbering scheme is restricted to those MOs formed from the valence atomic orbitals of C (2s,2p) F (2s,2p), Cl (3s, 3p), and Br (4s,4p). Vertical ionization potentials (IPs) of these orbitals taken from Cvitas *et al*.[3,4] are given in Tables 1 and 2. The three fluorine lone-pair atomic orbitals have symmetry $a_1 + a_2 + 2e$, whilst the chlorine or bromine lone pair has symmetry e. *Ab-initio* calculations using various basis sets[23] and measurements of the variation in the partial ionization cross-sections using synchrotron radiation[24] have allowed a qualitative description of the character of the individual valence MOs. Thus the 5e orbital is essentially comprised of a lone pair on the Cl or Br atom, and therefore the IP of this orbital changes substantially between CF_3Cl (13.08 eV) and CF_3Br (12.08 eV). The $5a_1$ orbital is associated with either C−Cl or C−Br bonding, so again its energy drops (by *ca*. 1 eV) between CF_3Cl and CF_3Br. The $1a_2$, 4e, 3e, and $4a_1$ orbitals are all essentially F 2p lone-pair orbitals, so their energies are invariant between CF_3Cl and CF_3Br although the small participation in C−F bonding character of these orbitals increases with increasing ionization energy. The 2e orbital is bonding on the CF_3 moiety, whereas the $3a_1$ orbital is both C−F and C−Cl/Br σ-bonding in character.[24] This overall assignment is confirmed by the similarity, both in relative intensities and peak positions, of the

TABLE 1: Energetics of Dissociation Channels of CF_3Cl and CF_3Cl^+

neutral/parent ion	dissociation channel	dissociation energy/eV[a]	vertical ionization energy/eV[b]
	$C^+ + 3F + Cl$	29.6	
$CF_3Cl^+\ \tilde{G}\ ^2A_1$			23.80
	$CF_2Cl + F^+$	22.63	
	$CF^+ + 2F + Cl$	21.83	
$\tilde{F}\ ^2E$			21.20
$\tilde{E}\ ^2A_1$			20.20
	$CF^+ + FCl + F$	19.27	
	$CF_2^+ + F + Cl$	19.03	
$\tilde{D}\ ^2E$			17.71
$\tilde{C}\ ^2E$			16.72
	$CF_3 + Cl^+$	16.68	
	$CF_2^+ + FCl$	16.47	
$\tilde{B}\ ^2A_2$			15.80
$\tilde{A}\ ^2A_1$			15.20
	$CF_2Cl^+ + F$	13.53[c]	
$CF_3Cl^+\ \tilde{X}\ ^2E$			13.08
	$CF_3^+ + Cl$	12.28	
	$CF + 2F + Cl$	12.73	
	$CF + FCl + F$	10.17	
	$CF_2 + F + Cl$	7.43	
	$CF_2Cl + F$	5.23[c]	
	$CF_2 + FCl$	4.87	
	$CF_3 + Cl$	3.68	
$CF_3Cl\ \tilde{X}\ ^1A_1$			0

[a] These data are calculated from the JANAF tables[25] for 0 K heats of formation and the following IPs: CF_3, 8.6 eV;[27] CF_2, 11.6 eV;[29] CF, 9.1 eV;[30] F, 17.4 eV;[25] Cl, 13.0 eV;[25] F_2, 15.7 eV.[31] [b] Cvitas *et al*.[3] [c] Calculated using a 0 K enthalpy of formation of CF_2Cl of -275 kJ mol^{-1} and an ionization potential of 8.3 eV.[26] Observed by PIMS with a threshold of 14.25 eV (Jochims *et al*.[5]). Powis[11] suggests a value of $<14.0 \pm 0.3$ eV.

TABLE 2: Energetics of Dissociation Channels of CF_3Br and CF_3Br^+

neutral/parent ion	dissociation channel	dissociation energy/eV[a]	vertical ionization energy/eV[b]
	$C^+ + 3F + Br$	29.0	
$CF_3Br^+\ \tilde{G}\ ^2A_1$			23.7
	$CF_2Br + F^+$	? + 17.4	
	$CF^+ + 2F + Br$	21.13	
$\tilde{F}\ ^2E$			20.9
$\tilde{E}\ ^2A_1$			19.8
	$CF^+ + FBr + F$	18.58	
	$CF_2^+ + F + Br$	18.33[c]	
$\tilde{D}\ ^2E$			17.57
$\tilde{C}\ ^2E$			16.55
$\tilde{B}\ ^2A_2$			15.85
	$CF_2^+ + FBr$	15.78	
	$CF_3 + Br^+$	14.78	
$\tilde{A}\ ^2A_1$			14.28
	$CF_2Br^+ + F$	14.01[d]	
$CF_3Br^+\ \tilde{X}\ ^2E$			12.08
	$CF_3^+ + Br$	11.58[e]	
	$CF + 2F + Br$	12.03	
	$CF + FBr + F$	9.48	
	$CF_2 + F + Br$	6.73	
	$CF_2Br + F$	?	
	$CF_2 + FBr$	4.18	
	$CF_3 + Br$	2.98	
$CF_3Br\ \tilde{X}\ ^1A_1$			0

[a] These data are calculated from the JANAF tables[25] for 0 K heats of formation and the following IPs: CF_3, 8.6 eV;[27] CF_2, 11.6 eV;[29] CF, 9.1 eV;[30] F, 17.4 eV;[25] Br, 11.8 eV;[25] F_2, 15.7 eV.[31] [b] Cvitas *et al*.[4] [c] Clay *et al*.[9] measure an AP of 18.02 ± 0.13 eV. [d] Appearance potential from Clay *et al*.[9] Heat of formation of the neutral not quoted in the JANAF tables[25] or Lias *et al*.[26] [e] Clay *et al*.[9] measure an AP of 11.56 ± 0.02 eV.

third to eighth bands in the He II photoelectron spectra of CF_3Cl and CF_3Br.[3,4] Spin−orbit structure is not resolved in any of the doubly-degenerate ^2E states of the parent ions, but vibrational structure is resolved for both CF_3Cl and CF_3Br in the fifth and sixth photoelectron bands (ionization to $\tilde{D}\ ^2E$ and $\tilde{E}\ ^2A_1$). In the $\tilde{D}$ state band of CF_3Cl^+, vibrational progressions of 1150, 720, and 360 cm^{-1} are observed[3] and assigned to ν_1 (a_1) or ν_4 (e) CF_3 stretching, ν_2 (a_1) CF_3 deformation, and ν_3 (a_1) C−Cl stretching modes, respectively. In the $\tilde{E}$ state band a single progression of 650 cm^{-1} is assigned to the ν_2 (a_1) CF_3 deformation mode. This mode is most likely to be excited upon ionization of a nonbonding F 2p lone-pair electron, justifying the qualitative assignment of the $4a_1$ orbital given above. For CF_3Br^+ [4] the $\tilde{D}$ state band shows just two partially-resolved progressions of 1080 and 690 cm^{-1}, corresponding to the ν_1/ν_4 and ν_2 vibrational modes involving the CF_3 moiety, whilst the $\tilde{E}$ state band shows the one vibrational progression (ν_2) of 620 cm^{-1}.

Since this paper will primarily be concerned with fragmentation of the different electronic states of CF_3Cl^+ and CF_3Br^+, the thermochemistry of the possible fragment ions needs to be known. Tables 1 and 2 also show the dissociation energies of the neutral and ionic fragments from CF_3X and CF_3X^+ (X = Cl, Br). The neutral channels are calculated from 0 K heats of formation given in the latest JANAF tables,[25] the values being *ca.* 0.05−0.10 eV higher if heats of formation at 298 K are used. For CF_2Cl, where no figure is quoted in the JANAF tables, we use a value of −275 kJ mol^{-1} recommended by Lias *et al.*[26] No value is available from either source for CF_2Br. The energies of the ion channels are calculated from these neutral-channel energies plus literature values for the ionization potentials (IPs) of the fragments (*e.g.* CF_3, CF_2). The values for $CF_2X^+ + F$ and $CF_3^+ + X$ warrant further comment. The IPs of CF_2Cl and CF_2Br have not been measured directly by photoelectron spectroscopy. For CF_2Cl we use a value of 8.3 eV quoted by Lias *et al.*[26] (obtained indirectly from observations of a near thermoneutral ion−molecule reaction involving this ion), giving a thermochemical threshold for $CF_2Cl^+ + F$ of 13.53 eV. The thermodynamic onset of this ion as measured by PIMS is 14.25 ± 0.05 eV (see later), but this technique will always give an upper limit to the (indirectly obtained) IP for CF_2Cl (9.02 eV). In his He I PEPICO study of fragmentation of the $\tilde{C}\ ^2E$ state of CF_3Cl^+ which fragments to CF_2Cl^+, analysis of the KERD led Powis[11] to suggest a thermochemical threshold for $CF_2Cl^+ + F$ of less than 14.0 ± 0.3 eV. In Table 1 we quote the Lias recommendation but note that this could be as much as 0.5 eV too low. For CF_2Br^+ we quote the appearance potential (AP = 14.01 eV) recently established by Clay *et al.*[9] in their PIMS study of CF_3Br. Since the neutral thermochemistry for CF_2Br is not known, we cannot extract an IP (CF_2Br) from this value. For dissociation to $CF_3^+ + X$, we use an IP for CF_3 of 8.6 eV.[27] This value comes from recent work on ion−molecule chemistry involving CF_3^+ and is substantially lower than both the values of 9.25 eV[28] (the recommended experimental value for the IP (CF_3) for many years prior to the work of Fisher *et al.*[27]) and of 8.98 eV[32] from a very recent *ab-initio* calculation. However, since ionization of CF_3 results in a large change from pyramidal to planar geometry, these are circumstances under which the onset of signal at the adiabatic IP is very difficult to determine. For comparison, in his PEPICO study Powis[11] calculated a dissociation energy for $CF_3^+ + Cl$ of 12.77 ± 0.17 eV and the best PIMS study at the time extrapolated to 0 K gave 12.81 ± 0.04 eV,[7] both values *ca.* 0.5 eV higher than that quoted in Table 1. Note, however, that, with the high improvement in sensitivity now available from modern synchrotron light sources and quadrupole detectors, the very recent PIMS study on CF_3Br by Clay *et al.*[9] measures an AP(CF_3^+) of 11.56 ± 0.02 eV, which is now in excellent agreement with the thermochemical energy for $CF_3^+ +$ Br of 11.58 eV (Table 2), calculated assuming an IP(CF_3) of 8.6 eV.

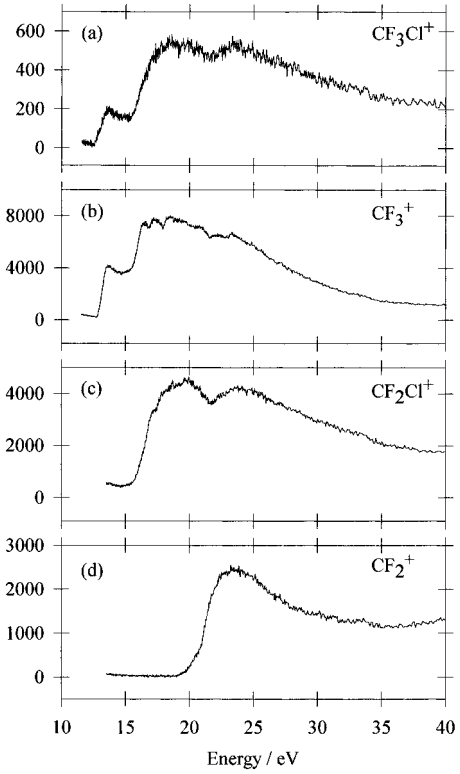

Figure 1. Photoionization yield curves for the four polyatomic molecular ions from CF_3Cl in the range 12−40 eV. The resolution is 4 Å or *ca.* 0.13 eV at 20 eV.

4. Electron−Ion Coincidence Studies of CF_3Cl^+ and CF_3Br^+

Ionic fragmentation of CF_3Cl excited by vacuum-UV radiation was studied between 12 and 40 eV. This large range in energy was covered in eight overlapping scans using the Seya monochromator at a fixed resolution of 4 Å. At each wavelength the signal was accumulated up to the same number of flux counts by the sodium salicylate/photomultiplier tube combination; therefore, it was possible to combine the separate scans. From the aggregated three-dimensional experimental data of coincidences *vs* TOF *vs* excitation wavelength, ion yield curves shown in Figure 1 are obtained. The main ion peaks observed are, in ascending order of threshold energy, CF_3Cl^+, CF_3^+, CF_2Cl^+, and CF_2^+.

We define and determine a threshold energy to be that value of the energy where the yield of a particular ion, within experimental error, lies above the background signal. The ion yield of CF_3Cl^+ (Figure 1a) shows a threshold at 12.52 ± 0.05 eV, which compares excellently with values from PIMS of 12.43,[6] 12.45,[5] and 12.39[7] eV. These values should be regarded as the most accurate estimate of the adiabatic IP of the $\tilde{X}\ ^2E$ ground state of CF_3Cl^+. The intensity of this ion channel is weak, mainly because the majority of the Franck−Condon region of the $\tilde{X}$ state potential surface lies above the $CF_3^+ +$ Cl dissociation channel and dissociates to this fragment ion (see Figure 3). A further enhancement in CF_3Cl^+ ion yield is seen around 15.2 eV, which corresponds to the vertical IP of the $\tilde{A}\ ^2A_1$ first excited state of CF_3Cl^+. At higher energies two broad

maxima are seen at 18 and 23 eV, and above 23 eV the CF_3-Cl^+ ion yield decreases slowly with increasing energy. For photon energies which can access several electronic states of CF_3Cl^+, the total cross section will have contributions from all these states weighted by their partial ionization cross sections, and the peaks at 18 and 23 eV are probably due to shape resonances caused by an enhanced cross section into one or more electronic states. These facts are in broad agreement with the measurements of total ionization cross sections from pseudophoton spectroscopy.[8]

The ion yield of CF_3^+ shows a sharp threshold at 12.75 ± 0.05 eV, again in good agreement with values from PIMS of 12.57,[6] 12.55,[5] and 12.65[7] eV. The thermochemical energy of $CF_3^+ + Cl$ lies as low as 12.28 eV if we accept the lowest literature value for the IP of CF_3 to be 8.6 eV. The CF_3^+ channel is by far the most intense in our spectrum, and the ion yield curve is very similar to that of Jochims *et al.*[5] As with the parent ion, the CF_3^+ yield is greatly enhanced at the IP of the first excited state of CF_3Cl^+, implying that this state fragments to this ion. Three smaller peaks are observed at 16.4, 17.3, and 18.4 eV before the CF_3^+ signal decreases at higher photon energies. These peaks are visible in the vacuum-UV absorption spectrum of CF_3Cl,[5] and their appearance in the CF_3^+ ion yield probably relates to the dissociation of autoionizing states of CF_3Cl. At any photon energy between 11 and 40 eV the relative yields of the ions can be determined from the values of the signals in Figure 1. Thus at 20.4 eV, the relative intensity of CF_3^+:CF_3Cl^+ is *ca.* 14:1 in our spectrum. This is very similar to the value obtained by Powis[11] at 21.2 eV of 13:1 but much smaller than the value of 40:1 quoted by Jochims *et al.*[5] The reason for this discrepancy between the two forms of TOF mass spectrometry and quadrupole detection could lie in the non-constant mass discrimination of many quadrupole spectrometers, whereas most TOF mass spectrometers (including our own) have a sensitivity which is approximately independent of mass. Note that such ratios represent the relative abundance of ions (parent and fragment) at a defined photon energy. This is different from a breakdown diagram which depicts the relative abundance of ions at a defined internal energy of the parent ion.[33]

The second most intense channel is due to CF_2Cl^+, and the threshold for this ion is measured to be 14.3 ± 0.2 eV (Figure 1c). The rise in the ion yield is slow near its onset, resulting in the relatively large uncertainty. This value is in exact agreement with that obtained by Jochims *et al.*[5] (14.25 eV) and by pseudophoton spectroscopy[8] (14.5 ± 0.5 eV). From a detailed analysis of the CF_3Cl^+ $\tilde{C}$ state KERD, Powis[11] revised the thermochemical energy of the $CF_2Cl^+ + F$ channel to be less than 14.0 ± 0.3 eV. The latest compilation of Lias *et al.*[26] suggests an energy for this channel as low as 13.53 eV (Table 1). Within error limits we believe that all these values are essentially the same and that CF_2Cl^+ turns on at an energy very close to its thermochemical value. The autoionizing structure observed by Jochims *et al.*[5] between 17 and 21 eV in the ion yield is seen in our spectrum, and the broad unresolved band at 25 eV (not covered by the spectrum in ref 5) could also be an effect due to autoionization, as it tallies with a feature in the photoabsorption oscillator strength spectrum of Zhang *et al.*[8] Ajello *et al.*[7] claim that CF_2Cl^+ is not the product of a direct photoionization process because the ion signal is proportional to the square of the gas pressure, and they favor a collision-induced dissociation mechanism involving CF_3Cl^+. However, our measurements (see later), together with those of Powis,[11] show that this ion originates primarily from fragmentation of the $\tilde{C}$ ^2E and $\tilde{D}$ ^2E states of the parent ion, making their suggestion very unlikely.

TABLE 3: Observed Thresholds (eV) of Photofragmentation Ions from CF_3Cl and CF_3Br

ion	Noutary[6]	Jochims *et al.*[5]	Ajello *et al.*[7]	Zhang *et al.*[8]	this work	lowest thermochemical threshold
CF_3Cl^+	12.43	12.45	12.39	12.5	12.52 ± 0.05	12.4−12.5[a]
CF_3^+	12.57	12.55	12.65	12.5	12.75 ± 0.05	12.28[b]
CF_2Cl^+		14.25		14.5	14.3 ± 0.2	13.53[c]
CF_2^+		18.85	18.84	19.0	18.9 ± 0.2	19.03[d]
Cl^+				19.5	20.0 ± 0.1	16.68
CF^+				23.0	22 ± 3	21.83[e]
C^+				33.0	32 ± 1	29.6[f]
F^+				34.0	32 ± 2	22.63[g]

ion	Noutary[6]	Clay *et al.*[9]	this work	lowest thermochemical threshold
CF_3Br^+	11.84	11.40 ± 0.01	11.63 ± 0.05	11.4−11.6[h]
CF_3^+		11.56 ± 0.02	11.92 ± 0.02	11.58[b]
CF_2Br^+		14.01 ± 0.06	14.5 ± 0.2	?
CF_2^+		18.02 ± 0.13	18.5 ± 0.2	18.33[i]
Br^+		15.69 ± 0.02	16.0 ± 1.5	14.78
CF^+			20 ± 2	21.13[j]
C^+			30 ± 3	29.0[k]

[a] Best estimate of the adiabatic IP of the $\tilde{X}$ ^2E state of CF_3Cl^+ from photoelectron spectroscopy.[3] [b] Assumes the lowest literature value for IP(CF_3) of 8.6 eV.[27] [c] Assumes the lowest literature value for IP(CF_2Cl) of 8.3 eV.[26] [d] Assumes the other products are F + Cl (see text). [e] Assumes the other products are 2F + Cl. [f] Assumes the other products are 3F + Cl. [g] Assumes the other product is CF_2Cl. [h] Best estimate of the adiabatic IP of the $\tilde{X}$ ^2E state of CF_3Br^+ from photoelectron spectroscopy.[4] [i] Assumes the other products are F + Br (see text). [j] Assumes the other products are 2F + Br. [k] Assumes the other products are 3F + Br.

The ion yield of CF_2^+ (Figure 1d) shows a threshold at 18.9 ± 0.2 eV, in excellent agreement with values from other PIMS studies of 18.85[5] and 18.84[7] eV. Pseudophoton spectroscopy yields 19.0 ± 0.5 eV.[8] These values are in good agreement with the thermochemical threshold to $CF_2^+ + F + Cl$ (19.03 eV), and we note that the threshold for this ion occurs in the Franck−Condon gap between the $\tilde{D}$ and $\tilde{E}$ states of the parent ion. The thermochemical threshold to $CF_2^+ + FCl$ lies much lower at 16.47 eV. The ion yield of CF_2^+ from CF_3Br shows a threshold at 18.5 ± 0.2 eV, close to the thermochemical threshold of $CF_2^+ + F + Br$ (18.33 eV) (see later), and therefore we assume that in both cases CF_2^+ forms in combination with the two atoms and not the diatomic neutral molecule.

Four weaker ions are observed at higher energies.[14] The Cl^+ ion shows a sharp threshold at 20.0 ± 0.1 eV, over 3 eV greater than the lowest thermochemical channel involving this ion. This energy coincides with that of the adiabatic IP of the $\tilde{E}$ $^2A_1$ state of CF_3Cl^+. At its peak of 22 eV the intensity of the Cl^+ signal is approximately half that of the peak of the CF_2^+ signal, in excellent quantitative agreement with the results from Zhang *et al.*[8] Much weaker peaks due to CF^+, F^+, and C^+ are also observed with threshold energies of 22 ± 3, 32 ± 1, and 32 ± 2 eV, respectively. The large errors on some of these values reflect the reduced signal strengths for these ions and hence the increased difficulty in measuring a threshold on top of a substantial background signal, but again these threshold values are in good agreement with those from pseudophoton spectroscopy.[8] For CF^+ and C^+ the threshold energies are in agreement with the calculated thermochemical limits involving these ions and atomic neutral products; for F^+ the experimental threshold is much higher (Table 1). All these threshold energies are collected in Table 3.

The ion yield curves of CF_3Br^+, CF_3^+, CF_2Br^+, and CF_2^+ from CF_3Br obtained with the same experimental conditions as for CF_3Cl are shown in parts a−d of Figure 2, respectively,

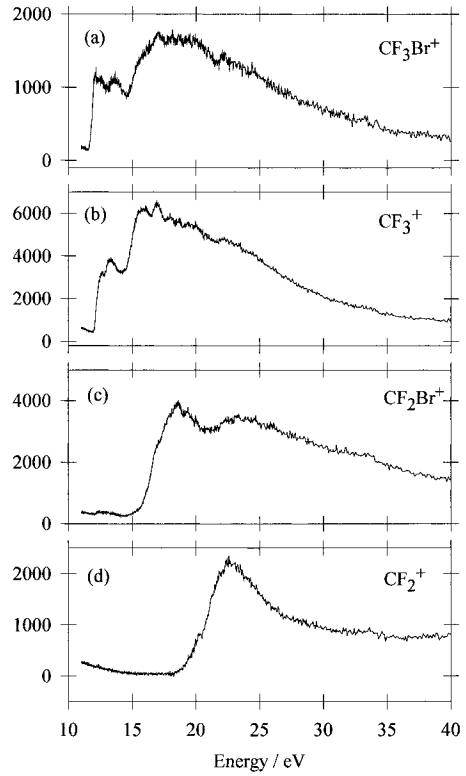

Figure 2. Photoionization yield curves for the four polyatomic molecular ions from CF_3Br in the range 11−40 eV. The resolution is 4 Å or *ca*. 0.13 eV at 20 eV.

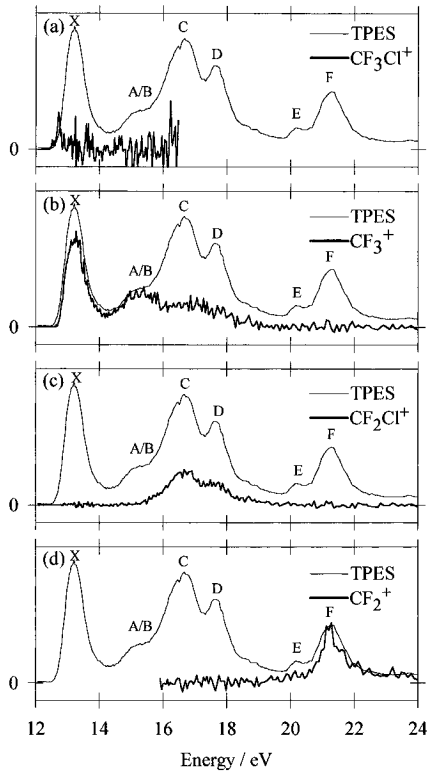

Figure 3. Threshold photoelectron spectrum and coincidence yields of (a) CF_3Cl^+, (b) CF_3^+, (c) CF_2Cl^+, and (d) CF_2^+ from CF_3Cl between 12 and 24 eV. The photon resolution is 4 Å or *ca*. 0.10 eV at 18 eV. The electronic states of CF_3Cl^+ ($\tilde{X}$, $\tilde{A}$, *etc*.) are marked.

and the threshold energies are reported in Table 3. There are only two other PIMS studies with which to compare our data: the early study by Noutary,[6] using vacuum-UV lab sources and a 1 m Seya−Namioka monochromator to generate tunable VUV radiation and a magnetic-sector mass spectrometer, and a very recent study by Clay *et al*.,[9] using monochromatized synchrotron radiation and quadrupole mass spectrometric detection. In general, there is a trend to lower appearance energies as the sensitivity of the detection systems improves with time. There have been no pseudophoton spectroscopic studies on CF_3Br. The shapes of the four ion yields in Figure 2 are very similar to those from CF_3Cl; however, a few comments should be made. First, although weak, the intensity of the parent ion signal is a larger fraction of the total ion signal than with CF_3Cl^+. This arises because a larger fraction of the Franck−Condon region of the $\tilde{X}\ ^2E$ state of CF_3Br^+ lies below the dissociation limit to $CF_3^+ + Br$ than for the equivalent region in CF_3Cl^+. Second, enhancements of both CF_3Br^+ and CF_3^+ ion yields occur around 14.3 eV near the vertical IP of the $\tilde{A}\ ^2A_1$ first excited state of CF_3Br^+. In the latter case this arises because the state-selected studies (see later) show that the CF_3Br^+ $\tilde{A}$ state fragments exclusively to $CF_3^+ + Br$. Third, for all the weaker ions such as CF_2^+ the signal at threshold shows a very slow rise with increasing energy. The higher sensitivity of quadrupole mass detection means that the values for the thresholds obtained by Clay *et al*.[9] are generally 0.3−0.5 eV lower than our values obtained by coincidence and TOF mass spectrometries. Fourth, the CF_2Br^+ ion likewise shows a slow rise at threshold (very similar to CF_2Cl^+), and again there is the maximum difference between the two values obtained by the different forms of PIMS. Note that neither the heat of formation of CF_2Br nor its IP has been measured directly, so these values for $AP(CF_2Br^+)$ cannot be compared with the thermochemical threshold. Fifth, unlike the Cl^+ threshold from CF_3Cl, that for Br^+ from CF_3Br does not rise steeply but is much more gradual near its onset. We can only determine its threshold energy (16.0 eV) to within ± 1.5 eV. It lies over 1 eV above the lowest dissociation channel involving this atomic ion.

5. State-Selected TPEPICO Studies of Fragmentation of CF_3Cl^+ and CF_3Br^+

TPEPICO spectra in the scanning mode were recorded for CF_3Cl^+ and CF_3Br^+ using the Seya and McPherson monochromators at resolutions of 4 and 2 Å, respectively. In the case of CF_3Cl^+ two overlapping scans were needed to cover the range 12−35 eV, where a fixed step size of *ca*. 2 Å was used. In the case of CF_3Br^+ four overlapping scans covered the energy range 11−23 eV and a fixed step size of *ca*. 0.03 eV was used. From the 3-D experimental data ion yields and TPE spectra can be obtained, and these are shown in Figures 3 and 4 for the main ions observed from CF_3Cl^+ and CF_3Br^+, respectively. We present the data in this way because we wish to show that the yields of individual ions generally correlate with different electronic states of the parent ion. Breakdown diagrams[33] show which fragmentation channels dominate at each photon energy and can readily be inferred from Figures 3 and 4. However, they are less instructive when many of the excited electronic states of the parent ions show nonstatistical fragmentation pathways (see section 6).

The CF_3Cl^+ ion yield is very weak and is only observable above the noise for the low-energy portion of the Franck−Condon zone of the $\tilde{X}$ state of CF_3Cl^+. The CF_3^+ ion yield follows the TPE signal through the $\tilde{X}$ and unresolved $\tilde{A}$ and $\tilde{B}$ states of CF_3Cl^+ and then decreases slowly to zero as the photon energy increases to *ca*. 20 eV. Unlike the observations of Powis,[11] we believe that there is a small but significant fragmentation of the $\tilde{C}\ ^2E$ and $\tilde{D}\ ^2E$ states of CF_3Cl^+ to CF_3^+, although the major fragmentation pathway is clearly to CF_2Cl^+ (Figure 3c). For CF_2Cl^+ the ion yield follows the TPE signal

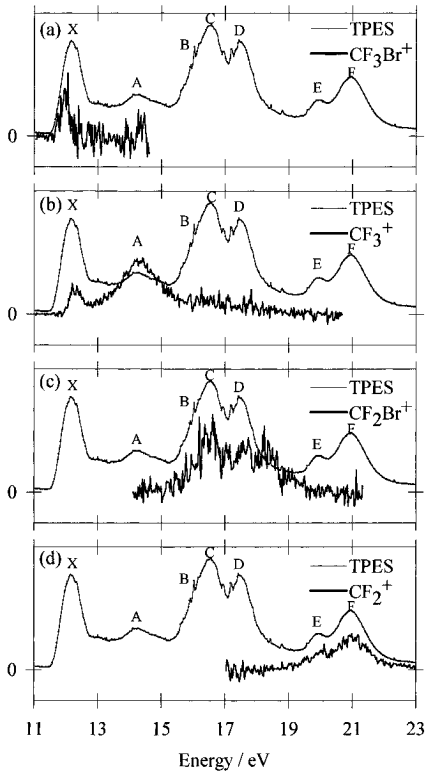

Figure 4. Threshold photoelectron spectrum and coincidence yields of (a) CF_3Br^+, (b) CF_3^+, (c) CF_2Br^+, and (d) CF_2^+ from CF_3Br between 11 and 23 eV. The photon resolution is 2 Å or *ca.* 0.05 eV at 18 eV. The electronic states of CF_3Br^+ ($\tilde{X}$, $\tilde{A}$, *etc.*) are marked.

TABLE 4: Mean KE Releases from Fragmentation of Valence States of CF_3Cl^+

daughter ion	parent ion	state	energy/eV	$\langle KE\rangle_t$/eV[a]	$\langle KE\rangle_t$/eV
CF_3^+	CF_3Cl^+	$\tilde{X}\ ^2E$	13.25	0.11 ± 0.01	
CF_3^+	CF_3Cl^+	$\tilde{A}\ ^2A_1$	15.20	0.88 ± 0.05	0.93[b]
CF_3^+	CF_3Cl^+	$\tilde{B}\ ^2A_2$	15.85	0.69 ± 0.11	
CF_2Cl^+	CF_3Cl^+	$\tilde{B}\ ^2A_2$	15.85	1.08 ± 0.23	
CF_3^+	CF_3Cl^+	$\tilde{C}\ ^2E$	16.55	0.68 ± 0.11	
CF_2Cl^+	CF_3Cl^+	$\tilde{C}\ ^2E$	16.55	1.24 ± 0.13	1.30[c]
CF_3^+	CF_3Cl^+	$\tilde{D}\ ^2E$	17.61	0.79 ± 0.10	
CF_2Cl^+	CF_3Cl^+	$\tilde{D}\ ^2E$	17.61	1.23 ± 0.12	1.30[d]
CF_2^+	CF_3Cl^+	$\tilde{F}\ ^2E$	21.28	0.61 ± 0.05[e]	
Cl^+	CF_3Cl^+	$\tilde{F}\ ^2E$	21.28	0.91 ± 0.06[f]	

[a] This work. Assumes Cl is a single isotope with mass 35.5 u. This approximation is valid because the difference in time-of-flight of the two chlorine isotopes of mass 35 and 37 u is less than the width of the peak as broadened by the KE release. [b] Evaluated from Figure 4d of ref 11. [c] Evaluated from Figure 7 of ref 11. [d] Value implied in ref 11 to have the same magnitude as for CF_2Cl^+ from CF_3Cl^+ $\tilde{C}\ ^2E$. [e] Assumes the other product is FCl. [f] Assumes the other product is CF_3.

through the Franck−Condon regions of the $\tilde{C}$ and $\tilde{D}$ states of CF_3Cl^+. For CF_2^+ (Figure 3d) the ion yield follows the TPE signal over the Franck−Condon region of the $\tilde{F}\ ^2E$, and possibly the $\tilde{E}\ ^2A_1$, state of the parent ion. For Cl^+ the signal is weak; however, the ion yield rises steeply at the adiabatic IP of the $\tilde{E}$ state and remains above zero through the Franck−Condon region of the $\tilde{E}$ and $\tilde{F}$ states of the parent ion. There is definitely a weak channel to this ion (in competition with CF_2^+) at the Franck−Condon maximum of the $\tilde{F}\ ^2E$ state (Table 4). The approximate thresholds for production of the four molecular ions can be deduced from Figure 3. In the case of CF_3Cl^+ and CF_3^+ they agree excellently with the values obtained from the non-state-selected experiments (section 4 and column 6 of Table 3). In the case of both CF_2Cl^+ and CF_2^+ the signal at threshold shows a very shallow rise, and the poorer signal-to-noise ratio

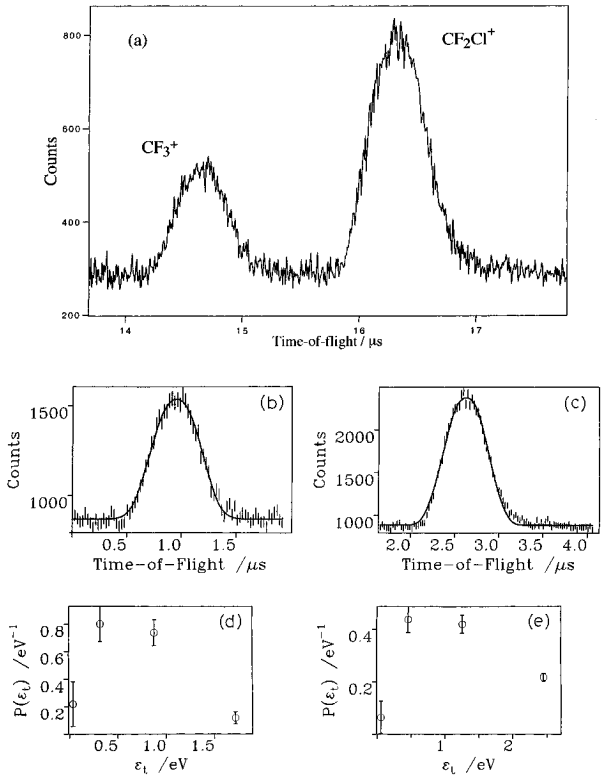

Figure 5. (a) Coincidence time-of-flight spectrum of CF_3^+ and CF_2Cl^+ from CF_3Cl photoionized at 17.61 eV into the $\tilde{D}\ ^2E$ state of the parent ion. The time resolution is 8 ns per channel, and the accumulation time is 8 h. (b and c) Simulations of the CF_3^+ and CF_2Cl^+ peaks using the method of Powis *et al.*[19] To improve the statistics of the fit, three successive datapoints are added. Zero time-of-flight corresponds to 13.7 μs in part a. (d and e) The probability distribution functions obtained from parts b and c (see text), yielding $\langle KE\rangle_t$ values of 0.79 ± 0.10 and 1.23 ± 0.12 eV, respectively.

of the ion yields in the state-selected experiments means that the error in the thresholds for these two ions is slightly greater than those obtained by the non-state-selected experiment.

Very similar results are obtained for state-selected fragmentation of the valence states of CF_3Br^+ (Figure 4). Now a larger portion of the Franck−Condon zone of the $\tilde{X}$ state of CF_3Br^+ lies below the dissociation threshold to $CF_3^+ + Br$. These rovibrational levels are stable with respect to dissociation, leading to a more pronounced parent ion signal than with CF_3Cl^+. The $\tilde{A}\ ^2A_1$ state of CF_3Br^+ fragments predominantly to CF_3^+ (Figure 4b) although there may be a very weak component to CF_2Br^+. The $\tilde{C}\ ^2E$ and $\tilde{D}\ ^2E$ states of the parent ion fragment predominantly to CF_2Br^+ (Figure 4c), but as with CF_3Cl^+ there is a small but significant branching ratio to CF_3^+ (the CF_3^+ yield has quite clearly *not* reduced to zero in the Franck−Condon zone of the $\tilde{C}$ and $\tilde{D}$ states (16−18 eV)). The $\tilde{F}\ ^2E$ and possibly $\tilde{E}\ ^2A_1$ states of CF_3Br^+ fragment exclusively to CF_2^+ (Figure 4d). The Br^+ yield is very weak but seems to follow the TPE signal over the $\tilde{E}$ state band of the parent ion and then drop to zero through the Franck−Condon region of the $\tilde{F}$ state. Unlike the CF_3Cl^+ $\tilde{F}$ state, there is not a dissociation route of CF_3Br^+ $\tilde{F}$ to Br^+ in competition with dissociation to CF_2^+.

TPEPICO spectra at fixed photon energies were measured at the Franck−Condon maxima of the majority of the valence states of CF_3Cl^+ and CF_3Br^+. A time resolution of 8 ns per channel was used in all these measurements. Data accumulation times were typically *ca.* 8−20 h per spectrum. Figure 5a shows the broadening of the CF_3^+ and CF_2Cl^+ peaks at 17.61 eV, the maximum of the CF_3Cl^+ $\tilde{D}\ ^2E$ state. Analytical expressions[34,35]

TABLE 5: Mean KE Releases from Fragmentation of Valence States of CF_3Br^+

daughter ion	parent ion	state	energy/eV	$\langle KE\rangle_t$/eV[a]	$\langle KE\rangle_t$/eV[b]
CF_3^+	CF_3Br^+	$\tilde{X}\ ^2E$	12.23	0.05 ± 0.03	
CF_3^+	CF_3Br^+	$\tilde{A}\ ^2A_1$	14.23	0.53 ± 0.04	0.60 ± 0.06
CF_2Br^+	CF_3Br^+	$\tilde{B}\ ^2A_2/\tilde{C}\ ^2E$	16.33	1.10 ± 0.14	
CF_2Br^+	CF_3Br^+	$\tilde{D}\ ^2E$	17.53	0.99 ± 0.13	
CF_2^+	CF_3Br^+	$\tilde{F}\ ^2E$	21.23	0.52 ± 0.04[c]	

[a] This work. Assumes Br is a single isotope with mass 80 u. This approximation is valid bacause the difference in time-of-flight of the two bromine isotopes of mass 79 and 81 u is less than the width of the peak as broadened by the KE release. [b] Reference 11. [c] Assumes the other product is FBr.

are available for obtaining the mean KE release for such peaks, although assumptions have to be made about the overall shape of the peak. We choose to use the method developed by Powis *et al.*[19] to extract a *distribution* of KE releases and hence a mean release for each peak. Such a method make no initial assumption about the overall peak shape. A set of TOF peaks, each with a discrete energy release, ϵ_t, is calculated. The number of components and the energy, ΔE, of the first member of the set depend primarily on the statistical quality of the data. The discrete energies are given by $\epsilon_t = (2n-1)^2\Delta E$, where $n = 1, 2, 3, ...$ A Gaussian tail is added to each rectangular TOF peak to allow for the effects of thermal broadening. The set of computed TOF peaks is obtained by performing Monte-Carlo trajectory calculations of ions through the TOF mass spectrometer. Inputs to the program include the masses of the parent and daughter ions, the geometry of the mass spectrometer, and the translational temperature of the parent ion both along and perpendicular to the axis of the apparatus. The coadded TOF peaks are then fitted to the experimental peak using a linear regression technique (Figure 5b and c). Outputs are the normalized probability distributions of ϵ_t (Figure 5d and e) and hence the mean KE release, $\langle KE\rangle_t$. The position of the peak in the $P(\epsilon_t)$ *vs* ϵ_t graph can also give information on the statistical or nonstatistical nature of the dissociation process, with nonstatistical processes exhibiting a maximum at larger values of ϵ_t than statistical processes.

In practice we only quote the values of $\langle KE\rangle_t$, and the results are shown in Tables 4 and 5 for CF_3Cl^+ and CF_3Br^+, respectively. The main reason for not interpreting the KERDs in more detail is the lack of cooling of the translational temperature, *T*, of molecules along the axis of the TPEPICO apparatus, since the molecules emerge from the inlet needle with little directionality.[15] With k_BT as high as 25 meV, this thermal effect degrades the detailed form of the TOF distribution. The only other measurements of KE releases have been made by Powis[11] for a limited number of the valence states of CF_3X^+, and his values for the mean KE releases are shown in Tables 4 and 5 for comparison. Note that, in the states that dissociate to CF_2^+, the analyses of the CF_2^+ time-broadened peaks have assumed that the other product is the diatomic neutral FX, even though the thresholds for CF_2^+ production (section 4) suggest that atomic products (F + X) are more likely to be associated with this ion. We have not attempted to apply the methods of Baer *et al.*[36] to determine whether fragmentation to $CF_2^+ + F + X$ is a simultaneous or a sequential process.

6. Discussion

The energy-scanning TPEPICO results for CF_3Cl^+ confirm what is to be expected from the thermochemistry of this system (Table 1). A very small portion of the ground state of CF_3Cl^+ is bound with respect to dissociation to $CF_3^+ + Cl$; only rovibrational levels of the parent ion below this dissociation limit can be supported, and it is these levels that give rise to the weak parent ion signal in the TPEPICO spectrum. Rovibrational levels of the $\tilde{X}$ state above this limit are unstable with respect to dissociation; therefore, the CF_3^+ daughter ion shows a threshold close to this dissociation limit and rises steeply in intensity above this energy. It is noticeable that our threshold for CF_3^+ production (12.75 ± 0.05 eV) from a coincidence experiment is greater than the values obtained from PIMS experiments (12.55−12.65 eV[5−7]) and that all values are *ca.* 0.4 eV above the thermochemical threshold value of 12.28 eV if the IP(CF_3) value of 8.6 eV[27] is accepted. These observations reflect both the reduced sensitivity of the former experiment and the difficulty of measuring the threshold of a fragment ion whose geometry (D_{3h} in the case of CF_3^+) is very different from that in the parent ion (C_{3v} for CF_3X^+). Our threshold for CF_2Cl^+ production (14.3 ± 0.2 eV) lies in the Franck−Condon gap between the $\tilde{X}$ and $\tilde{A}$ states of CF_3Cl^+, whereas thermochemistry suggests that it lies much lower (13.53 eV) in the high-energy tail of the $\tilde{X}$ state Franck−Condon zone. As with CF_3^+ we note the substantial difference between the theoretical and the observed threshold for production of this ion. The unresolved $\tilde{A}$ and $\tilde{B}$ states of CF_3Cl^+ dissociate almost exclusively to CF_3^+, whereas the $\tilde{C}$ and $\tilde{D}$ states dissociate predominantly to CF_2Cl^+. As remarked earlier, however, there is a definite channel to CF_3^+ from the $\tilde{C}$ and $\tilde{D}$ states of the parent ion (the branching ratio of this channel decreasing with increasing photon energy), whereas if there is a channel to CF_2Cl^+ from the $\tilde{A}/\tilde{B}$ states it is too weak to observe. The $\tilde{E}$ and $\tilde{F}$ states of CF_3Cl^+ dissociate predominantly to CF_2^+ (probably with F + Cl as the other products), and this fragment ion turns on at this thermochemical threshold, although there is a minor channel to Cl^+ presumably with CF_3 as the other product. Similar energy-scanning TPEPICO results have been obtained for CF_3Br^+ (the few differences having already been highlighted in section 5), and the comments above for CF_3Cl^+ pertain equally well to CF_3Br^+.

Perhaps the most interesting aspect of this work is related to the statistical *vs* dynamical nature of the dissociation of the valence states of CF_3Cl^+ and CF_3Br^+. Consider a general photodissociation $ABC^{(+)*} \rightarrow AB^{(+)} + C$, where C is an atom but $AB^{(+)}$ represents a polyatomic fragment (*e.g.* CF_3^+). There are two limiting extremes for such a photodissociation process. In one extreme, the photoexcited parent molecule is long-lived on a time period of internal motion (rotation and vibration) of the parent molecule so that any excess energy is partitioned statistically amongst the available degrees of freedom prior to dissociation. In this instance a relatively small amount of the excess energy is partitioned into translational motion of the products (the quantity that we measure in our experiments), with the majority being partitioned into internal energy of $AB^{(+)}$. As a general rule, $\langle KE\rangle_t$ decreases as the mass or complexity of the polyatomic molecule $AB^{(+)}$ increases. In the other extreme, $ABC^{(+)*}$ is so short-lived that dissociation occurs on a time scale which is comparable to or faster than that of internal molecular motion. Now a much greater fraction of the excess energy is partitioned into translational KE of the $AB^{(+)} + C$ products. These two extreme forms of photodissociation are called statistical[37] and impulsive.[38] In the former case, statistical theories (*e.g.* RRKM or quasi-equilibrium theory[39]) can be used to predict dissociation rates, and in general the details of the electronic state(s) to which $ABC^{(+)}$ is initially photoexcited are not important because internal conversion to the ground state is assumed to take place so rapidly that dissociation only occurs from this potential surface. In the latter case, dynamical or

TABLE 6: Comparison of Mean Energy Releases for F or Cl Loss from CF_3Cl^+ and CF_3Br^+ with Those Predicted from a Statistical and an Impulse Dissociation Model

daughter ion/neutral	parent ion and state	$\langle KE\rangle_t$/eV	E_{avail}/eV[a]	fraction$_{expt}$[b]	fraction$_{stat}$[c]	fraction$_{impulse}$[d]
CF_3^+	CF_3Cl^+ $\tilde{X}$	0.11(1)	0.97	0.11(1)	0.13	0.38
CF_3^+	CF_3Cl^+ $\tilde{A}$	0.88(5)	2.92	0.30(2)	0.13	0.38
CF_3^+	CF_3Cl^+ $\tilde{B}$	0.69(11)	3.57	0.19(4)	0.13	0.38
CF_3^+	CF_3Cl^+ $\tilde{C}$	0.68(11)	4.27	0.16(3)	0.13	0.38
CF_3^+	CF_3Cl^+ $\tilde{D}$	0.79(10)	5.33	0.15(2)	0.13	0.38
CF_2Cl^+	CF_3Cl^+ $\tilde{B}$	1.08(23)	2.32	0.47(9)	*ca*. 0.125	0.47
CF_2Cl^+	CF_3Cl^+ $\tilde{C}$	1.24(13)	3.02	0.41(4)	*ca*. 0.125	0.47
CF_2Cl^+	CF_3Cl^+ $\tilde{D}$	1.23(12)	4.08	0.30(3)	*ca*. 0.125	0.47
CF_3[e]	CF_3Cl^+ $\tilde{F}$	0.91(6)	4.60	0.20(1)	0.13	0.38
CF_3^+	CF_3Br^+ $\tilde{X}$	0.05(3)	0.65	0.08(5)	0.13	0.28
CF_3^+	CF_3Br^+ $\tilde{A}$	0.53(4)	2.65	0.20(2)	0.13	0.28
CF_2Br^+	CF_3Br^+ $\tilde{B}/\tilde{C}$	1.10(14)	2.32	0.47(6)	*ca*. 0.125	0.44
CF_2Br^+	CF_3Br^+ $\tilde{D}$	0.99(13)	3.52	0.28(4)	*ca*. 0.125	0.44

[a] The definition of E_{avail} for a late and early impulsive release of energy is given in section 6 of the text. For a statistical process, E_{avail} is simply the photon energy minus the dissociation energy (given in Tables 1 and 2). [b] Given by $\langle KE\rangle_t/E_{avail}$. It is assumed that all the error is in the experimental $\langle KE\rangle_t$ and none in E_{avail}, *i.e.* there is no error in the thermodynamic thresholds given in Tables 1 and 2. [c] Calculated from the phase space statistical theory due to Klots.[40] See eq I and section 6 of the text. [d] Calculated from the impulse dissociation model of Riley and Wilson.[38] See eq II and section 6 of the text. [e] Cl^+ is the ionic product.

impulsive theories can be used to calculate energy releases, and now the detailed topography of the potential energy surfaces from which dissociation occurs is crucial to interpret the dynamics.

Klots[40] has shown that for a statistical dissociation in which both energy and angular momentum are conserved, and where the excess or available energy is large enough that any activation or centrifugal barrier in the exit channel to dissociation products can be neglected, E_{avail} and the mean translational KE, $\langle KE\rangle_t$, released into the $AB^{(+)} + C$ products are related by a simple analytical expression:

$$E_{avail} = \frac{(r-1)}{2}\langle KE\rangle_t + \langle KE\rangle_t + \sum_i \frac{h\nu_i}{\exp\left(\frac{h\nu_i}{\langle KE\rangle_t}\right) - 1} \quad \text{(I)}$$

E_{avail} is given by the photon energy minus the energy of the $AB^{(+)} + C$ dissociation limit, r is the number of rotational degrees of freedom of the $AB^{(+)}$ product, and ν_i are the vibrational frequencies of the $AB^{(+)}$ fragment. For $CF_3X^+ \rightarrow CF_3^+ + X$ or $CF_2X^+ + F$ excess energies are typically greater than 1 eV (Table 6) and centrifugal barriers are small for long-range ion-induced dipole (Langevin) interactions;[37] therefore, the approximations of Klots[40] are valid and eq I can be applied. Conversely, for an impulsive dissociation Riley and Wilson[38] have shown that E_{avail} and $\langle KE\rangle_t$ are related by

$$\frac{\langle KE\rangle_t}{E_{avail}} = \text{fraction}_{impulse} = \frac{\mu_{A,B}}{\mu_{AB,C}} \quad \text{(II)}$$

where μ is a reduced mass. Thus for dissociation of CF_3Cl^+/CF_3Br^+ to CF_3^+ or CF_2Cl^+/CF_2Br^+, between 28 and 47% of the available energy is partitioned into translational energy of the products (the value depending on the mass combination of the products), substantially greater than the fractions calculated by phase space methods.[40] For all the photodissociation processes observed involving loss of a halogen atom, we compare the experimental fraction of the available energy channeled into translational energy of the products with that calculated by these two limiting models (Table 6). Two comments should be made about how some of this data is obtained. First, in calculating E_{avail} we use the lowest literature value for the $AB^{(+)} + C$ dissociation channel (the values in Tables 1 and 2). That is, it is assumed that the fragment ion, CF_3^+ or CF_2X^+, has relaxed to its new D_{3h} planar geometry at the moment of impulsive dissociation. This is termed a 'late' release of energy.[11] If the energy release is early, the fragment ion still retains some memory of its C_{3v} symmetry, and it can have up to 0.5 eV bound up in vibrational energy.[11] E_{avail} is therefore correspondingly reduced by *ca*. 0.5 eV, and the fraction observed in the translational energy of the products is somewhat higher than the values given in column 5 of Table 6. Second, in calculating the statistical fraction (column 6), we use the same vibrational frequencies for CF_3^+ as for the isoelectronic neutral molecule BF_3.[41] Note that, for a four-atom fragment, $r = 3$ and there are six vibrational frequencies of the fragment. Hence if $h\nu_i \ll \langle KE\rangle_t$ for all i, $E_{avail} = 8\langle KE\rangle_t$ or 12.5% of the available energy is channeled into translation. Vibrational frequencies for CF_2Cl^+ and CF_2Br^+ are not available, and we assume that this lower limit of energy is channeled into vibration (column 6); for dissociation to CF_3^+, the fraction is only slightly higher at 0.13.

At the level of accuracy of our experimental data, it is only appropriate to comment that dissociation of some valence states of CF_3X^+ seems to be more statistical than dynamical in character, or *vice-versa*. However, some patterns do emerge, which relate the bond that breaks to form the fragment ion + atom products wth the part of the parent molecule where ionization occurs. Dissociation of the ground state ($\tilde{X}$ ^2E) of CF_3Cl^+ and CF_3Br^+ has been studied in some detail by Powis and Danby,[10] and from an analysis of the detail of the KERDs they suggested that dissociation of these states to $CF_3^+ + X$ is essentially statistical in nature. By comparing the mean fraction of available energy deposited into translation with that of the two limiting theories, our data supports their analysis. Note that at the energies at which our measurements were taken dissociation to $CF_2X^+ + F$ is energetically closed. Consider now dissociation of the $\tilde{A}$ $^2A_1$ state of the two ions. Dissociation to both CF_3^+ and CF_2X^+ is energetically open, yet the only channel observed from the $\tilde{A}$ state of either ion is to $CF_3^+ + X$. For CF_3Cl^+ the fraction released into translation (0.30 ± 0.02) is closer to the prediction of the impulsive model than the statistical model, and if the impulsive dissociation is early, the fraction rises to *ca*. 0.36, very close to the impulsive prediction. For CF_3Br^+ $\tilde{A}$ the result is not quite so clear in that the experimentally-observed fraction (0.20 ± 0.02) lies midway between the limiting statistical and dynamical models. Ionization to the $\tilde{A}$ state involves removal of a σ-bonding C−X electron. Since this is the bond that breaks to give the $CF_3^+ +$

X products, it is perhaps not surprising that a statistical model does not fit the data at all well, and an impulsive dynamical model is more appropriate. Put another way, a consequence of such direct dynamics is that the $\tilde{A}$ state does not have time to couple efficiently with the ground state of the ion via internal conversion (the precursor to a statistical dissociation from the ground-state potential energy surface, the main assumption of quasi-equilibrium theory[39]); hence, the F atom loss channel to CF_2X^+, despite being energetically open, is not observed.

Neither the $\tilde{B}$ state of CF_3Cl^+ nor that of CF_3Br^+ is well resolved in the threshold photoelectron spectrum. In the former case it sits on the high-energy shoulder of the $\tilde{A}$ state band; in the latter it sits on the low-energy shoulder of the $\tilde{C}$ state band. It is therefore difficult to perform a true state-selected study on the fragmentation dynamics of this state. The $\tilde{B}$, $\tilde{C}$, and $\tilde{D}$ states of CF_3X^+ arise essentially from removal of a F lone-pair electron. At the energies of the $\tilde{C}$ and $\tilde{D}$ states dissociation to both CF_3^+ and CF_2X^+ is observed, although at the time Powis[11] was only able to observe the stronger CF_2X^+ channel.[42] This is surprising because at 16.55 and 17.61 eV, the Franck−Condon maxima of the $\tilde{C}$ and $\tilde{D}$ states of CF_3Cl^+, we measure the CF_3^+ yield to be *ca*. 30 and 40%, respectively, of the CF_2Cl^+ yield. For the $\tilde{B}$ and $\tilde{C}$ states of CF_3X^+, Table 6 shows that if the C−X bond breaks to form $CF_3^+ + X$, the fraction of energy released into translation is much closer to the statistical limit than to the impulse dynamical limit. Conversely, if a C−F bond breaks to form $CF_2X^+ + F$, then the fraction of the available energy released into translation is greater and is much closer to the impulsive limit of *ca*. 0.45. Given that the electron is removed from a F lone-pair orbital adjacent to a C−F bond, intuitively it seems sensible that the lifetime of the $\tilde{B}$ and $\tilde{C}$ electronic states of CF_3X^+ will be greater if the dissociation occurs through cleavage of the C−X bond than through cleavage of a C−F bond. Hence it is not surprising that dissociation to CF_3^+ shows a more statistical translational energy release than dissociation to CF_2X^+. However, for the $\tilde{D}$ state of both parent ions, whilst dissociation to $CF_3^+ + X$ is still essentially statistical, the fraction of translational KE released into $CF_2X^+ + F$ lies midway between the statistical and the impulsive limits (Table 6). This result is compatible with the increased CF_3 bonding character of the 3e molecular orbital compared to the 4e and $1a_2$ orbitals, because in the former case the charge is distributed over the whole of the CF_3 moiety rather than being localized on a F lone-pair atomic orbital. Powis[11] has commented that in other aspects F atom loss and dissociation of these excited states to CF_2X^+ is essentially a nonstatistical process. First, as we observe, dissociation is primaily to CF_2X^+ and *not* to the lower-energy CF_3^+ channel. This is an excellent example of the behavior of an isolated state and contradicts statistical theories which assume that internal conversion to the ground electronic state of the parent ion occurs very rapidly and prior to a much-slower dissociation process. Second, within a given electronic state Powis[11] found that $\langle KE \rangle_t$ is independent of vibrational excitation. This implies that the vibrational modes excited upon ionization are not strongly coupled to the reaction coordinate (*i.e*. intramolecular vibrational redistribution is slow), so that energy randomization cannot occur within the lifetime of the parent ion. Third, the shapes of the KERDs obtained by Powis and by us (Figure 5e) are suggestive of a fast and direct rather than a slow and statistical dissociation. Finally from Table 6, we note that the fraction of energy released into translational energy of the minor channel, $Cl^+ + CF_3$, from dissociation of the $\tilde{F}\ ^2E$ state of CF_3Cl^+ lies closer to the statistical than the impulsive limit. Given that the 2e orbital is bonding on the CF_3 moiety, fragmentation through cleavage of the C−Cl bond can only occur following a significant redistribution of energy within the molecule, conditions under which a statistical KE release into products is likely.

It is interesting to note that the dissociation of the $\tilde{A}\ ^2A_1$ and $\tilde{B}\ ^2E$ states of CH_3Cl^+ and CH_3Br^+ [12,43] shows many similarities but some differences to that of the $\tilde{A}$−$\tilde{D}$ states of CF_3Cl^+ and CF_3Br^+. First, dissociation of the $\tilde{A}$ state of CH_3Cl^+ proceeds by a nonstatistical single channel to $CH_3^+ + Cl$, even though the $CH_2Cl^+ + H$ channel lies lower in energy. Dissociation of the $\tilde{A}$ state of CH_3Br^+ to $CH_3^+ + Br$ is more statistical in character, although there are appearances in the KERDs of dynamical behavior for vibrationally-excited species. Dissociation of the $\tilde{B}$ state of both CH_3Cl^+ and CH_3Br^+ to CH_3^+ is essentially statistical, although there is a minor, highly nonstatistical channel to CH_2X^+. It is only in the recent work of Lane and Powis[12] that this minor channel to CH_2X^+ has been seen, it being unobserved in the initial PEPICO study of Eland *et al*.[43] Note that in this case the minor channel is through C−H bond cleavage to $CH_2X^+ + H$, whereas in the dissociation of the $\tilde{C}$ and $\tilde{D}$ states of CF_3X^+ the minor channel is through C−X bond cleavage to $CF_3^+ + X$. The $\tilde{A}$ state of CH_3X^+ arises from removal of a C−X σ-bonding electron, the $\tilde{B}$ state arises from removal of a C−H σ-bonding electron, and the arguments given in the preceding paragraph for CF_3X^+ can be used to rationalize many of these results for CH_3X^+. Perhaps the most surprising result is that when the C−H bond is weakened by electron removal to form the $\tilde{B}\ ^2E$ state of CH_3X^+, the dominant channel is not through C−H cleavage to $CH_2X^+ + H$ but following vibrational energy redistribution through C−X bond cleavage to $CH_3^+ + X$.

7. Conclusions

Using monochromatized synchrotron radiation we have performed fragmentation studies of the valence states of CF_3Cl^+ and CF_3Br^+ in the vacuum-UV (10−40 eV) with and without energy state selectivity of the photoelectrons. In the latter case, thresholds and yield curves are obtained for the fragment ions produced; in the former case the fragmentation pathway(s) of specific electronic states of CF_3X^+ is determined and the mean translational kinetic energy released into the products is measured. By comparing $\langle KE \rangle_t$ with the values predicted for the limiting extremes of a statistical and an impulsive dissociation process, we can infer the nature of the photodissociation dynamics. The parent ion signal is very weak, especially for CF_3Cl^+, because the majority of the $\tilde{X}$ state potential energy surface of both ions lies above the dissociation energy to $CF_3^+ + X$, and the kinetic energy data confirm that the dissociation dynamics of these states is essentially statistical. The first four excited valence states of CF_3X^+ fragment by halogen atom loss to either CF_3^+ or CF_2X^+. For the $\tilde{A}\ ^2A_1$ state, where removal of the electron occurs from a C−X bonding orbital, CF_3^+ is the dominant product with a large KE release suggestive of impulsive, nonstatistical dissociation dyanmics. For the $\tilde{B}\ ^2A_2$ and $\tilde{C}\ ^2E$ states, where removal of the electron occurs from a F lone-pair orbital, CF_2X^+ is the major product but with CF_3^+ as a substantial minor component. The energy releases to $CF_2X^+ + F$ suggest that this process is also essentially impulsive, whereas for dissociation to $CF_3^+ + X$ the KE releases are much closer to that predicted by statistical theories. For the $\tilde{D}\ ^2E$ fourth excited state the electron is removed from an orbital with more C−F bonding character than the 4e and $1a_2$ orbitals; now dissociation to CF_2X^+ is less impulsive in character, whilst dissociation to CF_3^+ remains statistical in nature. The fifth ($\tilde{E}\ ^2A_1$) and sixth ($\tilde{F}\ ^2E$) excited valence states of CF_3X^+ fragment mainly to CF_2^+. The

thresholds for this ion are very close to the thermochemical thresholds for production of CF_2^+ with two neutral atoms (F + X).

Since dynamical rather than statistical factors are dominating the fragmentation of many of the valence states of CF_3Cl^+ and CF_3Br^+, a complete understanding of these results needs detailed potential energy surfaces for the ground and excited states of these ions and how these surfaces evolve both adiabatically and diabatically into production of daughter ions. To the best of our knowledge, these calculations have not been carried out. Jahn−Teller interactions could also play a major role in the decay dynamics of excited states of *E* symmetry. These results, and similar results for CF_4^+ where nonstatistical effects dominate the fragmentation pathways of excited valence states,[18] suggest that the CF_3X molecules (X = F, Cl, Br) have not approached the 'large molecule' limit. If this were so, rapid internal conversion between the excited states would always lead to a statistical dissociation pattern occurring from the ground-state potential energy surface.[39] Since this is not the case, state-specific behavior is both expected and observed, the most striking example being the dissociation of the $\tilde{B}$, $\tilde{C}$, and $\tilde{D}$ excited states of CF_3X^+ to $CF_2X^+ + F$.

Acknowledgment. We thank the staff at the Daresbury Laboratory for considerable assistance, Dr. I. R. Lambert for help with some of the non-state-selected experiments, and Dr. I. Powis (Nottingham University) for helpful discussions and the use of his kinetic energy analysis program. The U.K. Engineering and Physical Sciences Research Council is thanked for an equipment grant, an Advanced Fellowship (P.A.H.), a Post-Doctoral Fellowship (D.M.S.), and Research Studentships (J.C.C. and K.R.Y.).

References and Notes

(1) Coburn, J. W. In *Plasma Etching and Reactive Etching*; Whetten, N. R., Ed.; American Institute of Physics: 1992.
(2) Molina, M. J.; Rowland, F. S. *Nature* **1974**, *249*, 810.
(3) Cvitas, T.; Gusten, H.; Klasinc, L. *J. Chem. Phys.* **1977**, *67*, 2687. Jadrny, R.; Karlsson, L.; Mattsson, L.; Siegbahn, K. *Phys. Scr.* **1977**, *16*, 235.
(4) Cvitas, T.; Gusten, H.; Klasinc, L.; Novak, I.; Vancik, H. *Z. Naturforsch.* **1978**, *33a*, 1528.
(5) Jochims, H. W.; Lohr, W.; Baumgartel, H. *Ber. Bunsen-Ges. Phys. Chem.* **1976**, *80*, 130.
(6) Noutary, C. J. *J. Res. Natl. Bur. Stand.* **1968**, *72A*, 479.
(7) Ajello, J. M.; Huntress, W. T.; Rayermann, P. *J. Chem. Phys.* **1976**, *64*, 4746.
(8) Zhang, W.; Cooper, G.; Ibuki, T.; Brion, C. E. *Chem. Phys.* **1991**, *151*, 343.
(9) Clay, J. T.; Walters, E. A.; Grover, J. R.; Willcox, M. V. *J. Chem. Phys.* **1994**, *101*, 2069.
(10) Powis, I.; Danby, C. J. *Chem. Phys. Letts.* **1979**, *65*, 390.
(11) Powis, I. *Mol. Phys.* **1980**, *39*, 311.
(12) Lane, I. C.; Powis, I. *J. Phys. Chem.* **1993**, *97*, 5803.
(13) Creasey, J. C.; Lambert, I. R.; Tuckett, R. P., Frasinski, L. J.; Hatherly, P. A.; Stankiewicz, M.; Holland, D. M. P. *J. Chem. Phys.* **1990**, *93*, 3295.
(14) Creasey, J. C. Ph.D. Thesis, University of Birmingham, 1992.
(15) Hatherly, P. A.; Stankiewicz, M.; Codling, K.; Creasey, J. C.; Jones, H. M.; Tuckett, R. P. *Meas. Sci. Technol.* **1992**, *3*, 891.
(16) Wiley, W. C.; McClaren, I. H. *Rev. Sci. Instrum.* **1955**, *26*, 1150.
(17) Stankiewicz, M.; Hatherly, P. A.; Frasinski, L. J.; Codling, K.; Holland, D. M. P. *J. Phys. B.* **1989**, *22*, 21.
(18) Smith, D. M.; Tuckett, R. P.; Yoxall, K. R.; Codling, K.; Hatherly, P. A.; Aarts, J. F. M.; Stankiewicz, M. *J. Chem. Phys.* **1994**, *101*, 10559.
(19) Powis, I.; Mansell, P. I.; Danby, C. J. *Int. J. Mass. Spectrom. Ion Phys.* **1979**, *32*, 15.
(20) Creasey, J. C.; Lambert, I. R.; Tuckett, R. P.; Hopkirk, A. *Mol. Phys.* **1990**, *71*, 1367.
(21) Creasey, J. C.; Hatherly, P. A.; Lambert, I. R.; Tuckett, R. P. *Chem. Phys. Lett.* **1992**, *188*, 223.
(22) Biehl, H.; Boyle, K. J.; Smith, D. M.; Tuckett, R. P. *Chem. Phys. Lett.*, to be submitted.
(23) Popkie, H. E.; Kaufman, J. J. *Int. J. Quantum Chem., Symp.* **1977**, *11*, 433.
(24) Bozek, J. D.; Bancroft, G. M.; Cutler, J. N.; Tan, K. H.; Yates, B. W.; Tse, J. S. *Chem. Phys.* **1989**, *132*, 257.
(25) Chase, M. W.; Davies, C. A.; Downey, J. R.; Frurip, D. J.; McDonald, R. A.; Syverud, A. N. *J. Phys. Chem. Ref. Data* **1985**, *14*, suppl no. 1.
(26) Lias, S. G.; Bartmess, J. E.; Liebman, J. F.; Holmes, J. L.; Levin, R. D.; Mallard, W. G. *J. Phys. Chem. Ref. Data* **1988**, *17*, suppl no. 1.
(27) Fisher, E. R.; Armentrout, P. B. *Int. J. Mass Spectrom. Ion Proceses* **1990**, *101*, R1.
(28) Lifshitz, C.; Chupka, W. A. *J. Chem. Phys.* **1967**, *47*, 3439.
(29) Dyke, J. M.; Golab, L.; Jonathan, N.; Morris, A.; Okuda, M. *J. Chem. Soc., Faraday Trans. 2* **1974**, *70*, 1828.
(30) Dyke, J. M.; Lewis, A. E.; Morris, A. *J. Chem. Phys.* **1984**, *80*, 1382.
(31) van Lonkhuyzen, H.; de Lange, C. A. *Chem. Phys.* **1984**, *89*, 313.
(32) Horn, M.; Oswald, M.; Oswald, R.; Botschwina, P. *Ber. Bunsen-Ges. Phys. Chem.* **1995**, *99*, 323.
(33) Berkowitz, J. *Photoabsorption, photoionisation and photoelectron spectroscopy*; Academic Press: New York, 1979.
(34) Franklin, J. L.; Hierl, P. M.; Whan, D. A. *J. Chem. Phys.* **1967**, *47*, 3148.
(35) Stockbauer, R. *Int. J. Mass Spectrom. Ion Processes* **1977**, *25*, 89.
(36) Baer, T.; dePristo, A. E.; Hermans, J. J. *J. Chem. Phys.* **1982**, *76*, 5917.
(37) Baer, T. *Adv. Chem. Phys.* (Prigogine, I., Rice, S. A., Eds.) **1986**, *LXIV*, 111.
(38) Riley, S. J.; Wilson, K. R. *J. Chem. Soc., Faraday Discuss.* **1972**, *53*, 132.
(39) Rosenstock, H. M. *Adv. Mass Spectrom.* **1968**, *4*, 523.
(40) Klots, C. E. *J. Chem. Phys.* **1973**, *58*, 5364.
(41) Herzberg, G. *Electronic Spectroscopy of Polyatomic Molecules*; Van Nostrand Reinhold Co.: New York, 1966.
(42) Following a reanalysis of his original data, Powis (private communication, 1995) now believes that the CF_3^+ signal was present, albeit weakly, at the energies of the B, C, and D states of CF_3X^+.
(43) Eland, J. H. D.; Frey, R.; Kuestler, A.; Schulte, H.; Brehm, B. *Int. J. Mass Spectrom. Ion Phys.* **1976**, *22*, 155.

JP952318X